

# Validity/invalidity of Schottky-Mott rules for Schottky contacts to III-V nitride semiconductor heterostructures

Changzhi Lu

Department of Electronic Information and Control Engineering, Beijing University of Technology, Beijing 100022, Peoples Republic of China

S. Noor Mohammad<sup>a)</sup>

Department of Electrical and Computer Engineering, Howard University, Washington, DC 20059 and  
Department of Materials Science and Engineering, University of Maryland, College Park, Maryland 20742

(Received 14 June 2006; accepted 17 August 2006; published online 20 October 2006)

Carrier transport through the metal/semiconductor and metal/semiconductor/semiconductor (*M/S/S*) Schottky contact interfaces has been studied. Metal/*n*-GaN, metal/*n*-Al<sub>x</sub>Ga<sub>1-x</sub>N, and metal/*n*-Al<sub>x</sub>Ga<sub>1-x</sub>N/*n*-GaN diodes have been chosen for the study. It has been observed that, owing to the presence of the piezoelectric polarization field and a quantum well at the Al<sub>x</sub>Ga<sub>1-x</sub>N/GaN interface, the Al<sub>x</sub>Ga<sub>1-x</sub>N/GaN contacts exhibit properties distinctly different from those of the Al<sub>x</sub>Ga<sub>1-x</sub>N contacts. The superiority of the Al<sub>x</sub>Ga<sub>1-x</sub>N/GaN contacts to that of the Al<sub>x</sub>Ga<sub>1-x</sub>N contacts largely disappears at high temperatures. While the GaN and Al<sub>x</sub>Ga<sub>1-x</sub>N contacts appear to obey the Schottky-Mott rule, the Al<sub>x</sub>Ga<sub>1-x</sub>N/GaN contacts tend to disobey it. © 2006 American Institute of Physics. [DOI: 10.1063/1.2358956]

In this investigation we attempt to study high temperature Schottky-Mott characteristics of metal/GaN (S1), metal/Al<sub>x</sub>Ga<sub>1-x</sub>N (S2), and metal/Al<sub>x</sub>Ga<sub>1-x</sub>N/GaN (S3) diodes and to shed light on the validity/invalidity of Schottky-Mott rule for them. To our knowledge, no efforts have so far been made to address this rule for the *M/S/S* diodes. The dependence of room-temperature electron affinity  $\chi_S$  on the Al mole fraction  $x$  of Al<sub>x</sub>Ga<sub>1-x</sub>N may be given by<sup>1</sup>  $\chi_S(\text{Al}_x\text{Ga}_{1-x}\text{N}) = \chi_S(\text{GaN}) - m_S x$ , where  $\chi_S(\text{GaN}) = 4.31$  eV and  $m_S = 0.9$  eV. Thus  $\chi_S(\text{Al}_{0.2}\text{Ga}_{0.8}\text{N}) = 4.13$  eV, as determined from the room-temperature plot presented earlier.<sup>2</sup> The famous Schottky-Mott rule<sup>3</sup> predicts that barrier height  $\phi_B$  is equal to the difference between the electron affinity  $\chi_S$  of the semiconductor and the work function  $\phi_M$  of the metal. More specifically, if  $E_G$  is the semiconductor energy band gap, then  $q\phi_B = q\phi_M - \chi_S$  for contacts to *n* semiconductor and  $q\phi_B = (\chi_S + E_G) - q\phi_M$  for contacts to *p* semiconductor.

Semiconductor layers were grown on 400  $\mu\text{m}$  thick (0001) sapphire substrate by metal-organic chemical vapor deposition method. For the S3 diodes, 60 nm thick GaN buffer layer was first grown on sapphire substrate. It was followed successively by the growth of a 2  $\mu\text{m}$  thick undoped GaN, a 5 nm thick undoped Al<sub>x</sub>Ga<sub>1-x</sub>N, a 10 nm thick ( $5.0 \times 10^{18} \text{ cm}^{-3}$ ) Si-doped Al<sub>x</sub>Ga<sub>1-x</sub>N, and finally a 5 nm thick ( $1.0 \times 10^{19} \text{ cm}^{-3}$ ) Si-doped GaN. For the S2 diodes, 60 nm thick GaN buffer layer was first grown on 400  $\mu\text{m}$  thick sapphire substrate. It was followed successively by the growth of a 1  $\mu\text{m}$  thick lowly Si-doped ( $\sim 1.0 \times 10^{17} \text{ cm}^{-3}$ ) Al<sub>x</sub>Ga<sub>1-x</sub>N and a 5 nm thick ( $5.0 \times 10^{18} \text{ cm}^{-3}$ ) Si-doped GaN. For the S1 diode, a 1  $\mu\text{m}$  thick lowly Si-doped ( $\sim 1.0 \times 10^{17} \text{ cm}^{-3}$ ) GaN was grown on the substrate. The growth temperatures were 1010 °C for GaN and 1070 °C for Al<sub>x</sub>Ga<sub>1-x</sub>N ( $x=0.2$ ). The flows of trimethyl aluminum

and trimethyl gallium were adjusted over time to achieve Al<sub>x</sub>Ga<sub>1-x</sub>N ( $x=0.20$ ). The flow of silane was adjusted to achieve *n* doping of semiconductors.

Several samples were cut from each wafer and cleaned by degreasing in a soap solution followed by 3 min ultrasonic baths ( $T=27$  °C) successively in trichloroethylene, acetone, and methanol. The samples were then dipped in a heated bath ( $T=70$  °C) of  $\text{NH}_4\text{OH}:\text{H}_2\text{O}_2:\text{H}_2\text{O}$  (1:1:5) mixture for 3 min, followed by a 3 min dip in a heated  $\text{HCl}:\text{H}_2\text{O}_2:\text{H}_2\text{O}$  (1:1:5) mixture ( $T=70$  °C). They were rinsed in de-ionized water after the acid treatment.

The  $\text{NH}_4\text{OH}:\text{H}_2\text{O}_2:\text{H}_2\text{O}$  (1:1:5) mixture does not generally remove the oxide/hydroxide layers completely from throughout the surface. So, to overcome this problem, samples were cleaned using aqua regia ( $\text{H}_2\text{O}:\text{HNO}_3:\text{HCl} = 1:2:6$ ) and then de-ionized water. They were kept immersed in methanol during the idle time of processing after aqua regia treatment to avert subsequent oxide/hydroxide formation. Schottky diodes were fabricated using two-step photolithography.<sup>2</sup> The Ohmic contact was the Ti/Al/Pd/Au (200 Å/600 Å/400 Å/500 Å) multilayer contact, and the Schottky contact was the bilayer Ni/Au (1000 Å/300 Å) contact. For both S2 and S3 diodes, Schottky barrier heights and ideality factors were measured<sup>4</sup> by current-voltage (*I-V*) and capacitance-voltage (*C-V*) methods as functions of temperature *T*.

Figure 1(a) compares the *I-V* based Schottky barrier height  $\phi_B$  of the S2 and S3 diodes. As evident from Fig. 1(a), the measured variation of  $\phi_B$  with *T* for the S3 diodes is opposite to that for the S2 Schottky diodes. For the S2 diodes,  $\phi_B$ , as determined for 26, 100, 150, 200, 250, and 300 °C, are 1.03, 0.95, 0.83, 0.72, 0.59, and 0.49 V, respectively. For the S3 diodes,  $\phi_B$ , as determined for 26, 100, 150, 200, 250, and 300 °C, are 0.762, 0.835, 0.973, 1.104, 1.233, and 1.321 V, respectively. The S3 diodes have quantum well and two-dimensional electron gas (2DEG) at the Al<sub>x</sub>Ga<sub>1-x</sub>N/GaN interface. As a result, some of the thermally activated metal electrons, while trying to tunnel into the

<sup>a)</sup> Author to whom correspondence should be addressed; also at: Electronic Science and Technology Division, U.S. Naval Research Laboratory, Washington, DC 20375; electronic mail: snmohammad2002@yahoo.com and snmd@umd.edu

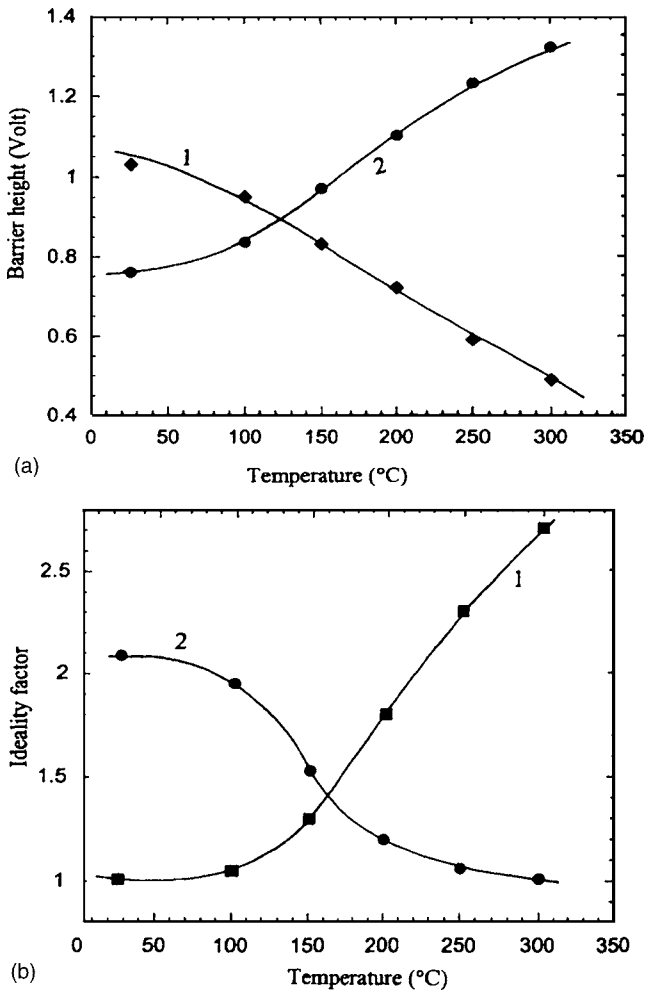


FIG. 1. Temperature dependence of the Schottky diode (a) barrier height and (b) ideality factor for the Al<sub>x</sub>Ga<sub>1-x</sub>N and Al<sub>x</sub>Ga<sub>1-x</sub>N/GaN diodes. Curve 1 is for the Al<sub>x</sub>Ga<sub>1-x</sub>N diode and curve 2 is for the Al<sub>x</sub>Ga<sub>1-x</sub>N/GaN diode.

semiconductor, are nullified by the polarized induced positive charges; others are transported into the quantum well(s). More Al<sub>x</sub>Ga<sub>1-x</sub>N donor atoms are thus ionized at higher  $T$ , and the free electrons, thus created, are drifted into the quantum well. The  $M/S$  depletion region is consequently widened, and  $\phi_B$  enlarged. The  $\phi_B$  thus becomes higher than what it should otherwise be under normal circumstances. This effect is absent in the S2 and S1 diodes.

Figure 1(b) depicts the temperature dependent ideality factor  $n_{idl}$  obtained from  $I$ - $V$  plots. For the S3 Schottky diodes,  $n_{idl}$  decreases with increasing  $T$ . But, for the S2 Schottky diodes, it increases with increasing  $T$ . Such an increase in  $n_{idl}$  with  $T$  was found also for the Pt/ $n$ -GaN Schottky contacts.<sup>5</sup> Transport mechanisms such as trap-assisted tunneling, field emission, and thermionic field emission are very highly sensitive to  $\phi_B$ . They decrease almost exponentially with increasing  $\phi_B$ . So, for the S2 Schottky diodes, for which  $\phi_B$  decreases with increasing  $T$ , the forward current  $I_F$  is dominated by these transport mechanisms more at  $T > 300$  K than at  $T = 300$  K. Consequently  $n_{idl}$  is larger at higher  $T$ . In contrast, for the S3 Schottky diodes, for which  $\phi_B$  increases with increasing  $T$ ,  $I_F$  is hardly affected by these transport mechanisms at higher  $T$ . The ideality factor  $n_{idl}$  is, therefore, far smaller at  $T > 300$  K than at  $T = 300$  K.

The electron affinity  $\chi_S$  of a semiconductor is the energy difference between the vacuum level and its conduction band edge  $E_C$ . Chen and Lue<sup>6</sup> found that  $\chi_S$  is essentially independent of  $T$  for  $0 \text{ K} \leq T \leq 300 \text{ K}$ . The temperature dependence of this  $\chi_S$  may be estimated also from temperature dependent conduction band edge of the semiconductor. For this, the temperature dependent energy band gap of GaN and AlN may be assumed to have the form<sup>7</sup>

$$E_G(T) = E_G(0) - \alpha_G T^2 / (T + T_G), \quad (1)$$

where  $E_G(0)$  is the energy band gap at 0 K, and  $\alpha_G$  and  $T_G$  are fitting parameters.  $E_G(0) = 3.48 \text{ eV}$ ,  $\alpha_G = 1.08 \text{ meV/K}$ , and  $T_G = 745 \text{ K}$  for GaN;  $E_G(0) = 6.29 \text{ eV}$ ,  $\alpha_G = 1.80 \text{ meV/K}$ , and  $T_G = 1462 \text{ K}$  for AlN. If  $E_{GA} \equiv E_G(\text{Al}_x\text{Ga}_{1-x}\text{N})$ ,  $E_{GB} \equiv E_G(\text{AlN})$ , and  $E_{GC} \equiv E_G(\text{GaN})$ , then the energy band gap of Al<sub>x</sub>Ga<sub>1-x</sub>N, as a function of Al mole fraction  $x$  and the temperature  $T$ , may be given by<sup>8</sup>

$$E_{GA}(x, T) = xE_{GB}(T) + (1-x)E_{GC}(T) - bx(1-x), \quad (2)$$

where  $E_{GB}(300 \text{ K}) = 6.20 \text{ eV}$ ,  $E_{GC}(300 \text{ K}) = 3.39 \text{ eV}$ , and  $b = 1.0 \pm 0.3 \text{ eV}$ . Equation (2), together with Eq. (1), gives  $E_G(\text{Al}_x\text{Ga}_{1-x}\text{N})$  as a function of  $T$ . This  $E_G$  shrinks at higher  $T$ . If it is assumed that the conduction band edge  $E_C$  shifts downward, the valence band edge  $E_V$  shifts upward during this shrinkage, and that these two shifts are equal and opposite, then  $\chi_S(T)$  of Al<sub>x</sub>Ga<sub>1-x</sub>N, with respect to that at  $T = 300 \text{ K}$ , may be

$$\chi_S(T) = \chi_S(300 \text{ K}) + [E_G(T) - E_G(300 \text{ K})]/2 \text{ (eV)}. \quad (3)$$

The variation of  $\chi_S(T)$  with  $T$  is shown in Fig. 2. It indicates that, following the same trend, as suggested by Chen and Lue,<sup>6</sup>  $\chi_S(T)$  for Al<sub>x</sub>Ga<sub>1-x</sub>N is quite insensitive to  $T$ . For  $26^\circ \text{C} \leq T \leq 300^\circ \text{C}$ , the change in  $\chi_S(T)$  is only  $0.09 \text{ eV}$ .

For S2 diodes, an increase in  $T$  accompanies an increase in energy of the metal electrons and hence a decrease in  $\phi_M$ . Although, at higher  $T$ , there occurs some increase in  $\chi_S$ , this increase is small. As a result, in line with the Schottky-Mott rule,  $\phi_B$ , at higher  $T$ , decreases with decreasing  $\phi_M$ . For the same reason,  $\phi_M$  for the S3 diodes is also lower at higher  $T$ . Metal electrons, at these temperatures, have additionally higher energy and higher coupling with the Al<sub>x</sub>Ga<sub>1-x</sub>N surface electrons, which affect the polarization charges  $\sigma_p$  of the Al<sub>x</sub>Ga<sub>1-x</sub>N surface. Band structure diagram for the S3 diodes is shown in Fig. 3. The diagram indicates that polarization charges  $-\sigma_p$  of the quantum well is consequently affected, and the sheet carrier concentration of the 2DEG is reduced. A reduction of the sheet carrier concentration of the 2DEG promotes drift of electrons from Al<sub>x</sub>Ga<sub>1-x</sub>N into the quantum well, creating larger number of ionized donor atoms and wider depletion region. The  $\phi_B$  value is consequently increased. So, at higher  $T$ , both  $\phi_B$  and  $\chi_S$  increase, but  $\phi_M$  decreases. Consequently the Schottky-Mott rule  $q\phi_B = q\phi_M - \chi_S$  is hardly obeyed. To our knowledge, this is a very important observation made for the S3 diodes for the first time. It strongly suggests that any modification of a  $M/S$  structure interfering the charge alignment at its  $M$  and  $S$  faces tends to undo the validation of the rule:  $q\phi_B = q\phi_M - \chi_S$ .

In order to determine whether the temperature dependent changes in  $\phi_B$  and  $n_{idl}$  resulted from structural changes at the interface, an investigation of the reversibility of these measurements was conducted. For this,  $I_F$  vs  $V$  plot for the A<sub>0</sub>

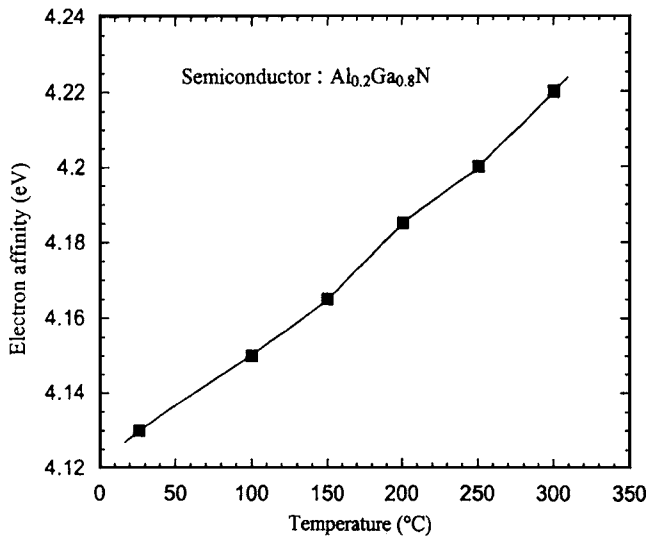


FIG. 2. Calculated variation of metal electron affinity modified by high temperature chemistry.

and  $B_0$  diodes was performed.  $A_0$  diodes are the S3 diodes kept at  $T=26^\circ\text{C}$  all the time.  $B_0$  diodes are the S3 diodes, which underwent a stepwise heating process being kept at each temperature step for about 15 min. More specifically, the device temperature was increased stepwise from  $T=26$  to  $50^\circ\text{C}$ , from  $50$  to  $150^\circ\text{C}$ ; from  $150$  to  $200^\circ\text{C}$ , and finally from  $200$  to  $300^\circ\text{C}$ , respectively. The devices were then cooled down back to  $26^\circ\text{C}$ . So, the  $B_0$  diodes underwent some form of thermal annealing. The forward currents for the  $A_0$  and  $B_0$  diodes, shown in Fig. 4, were obtained at  $26^\circ\text{C}$ . As may be noted from Fig. 4, these currents for the  $B_0$  diodes are lower than those for the  $A_0$  diodes. This might be due to the 2DEG sheet charge density for the  $B_0$  diodes being lower than that for the  $A_0$  diodes. The  $\phi_B$  for the  $B_0$  diodes was, however, higher than that for the  $A_0$  diodes. The difference between the two might have resulted from different interfacial reactions and/or diffusion processes at high  $T$ ,

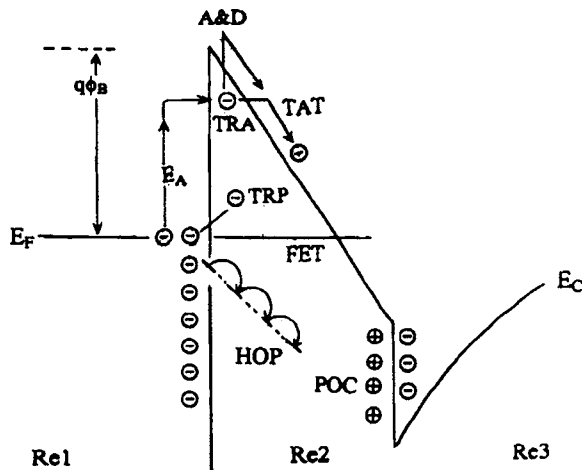


FIG. 3. Schematic diagram showing charge alignment due to polarization effect, two-step trap-assisted tunneling, field-emission tunneling, trapping, and hopping, in the interface regions of  $\text{Al}_x\text{Ga}_{1-x}\text{N}/\text{GaN}$  Schottky diodes. In the figure activation energy is denoted by  $E_A$ , deep level trapping by TRP, shallow-level trapping by TRA, two-step trap-assisted tunneling by TAT, activation and drift by A&D, field-emission tunneling by FET, hopping by HOP, polarization charge by POC, metal region 1 by RE1,  $\text{Al}_x\text{Ga}_{1-x}\text{N}$  region 2 by RE2, and GaN region 3 by RE3.

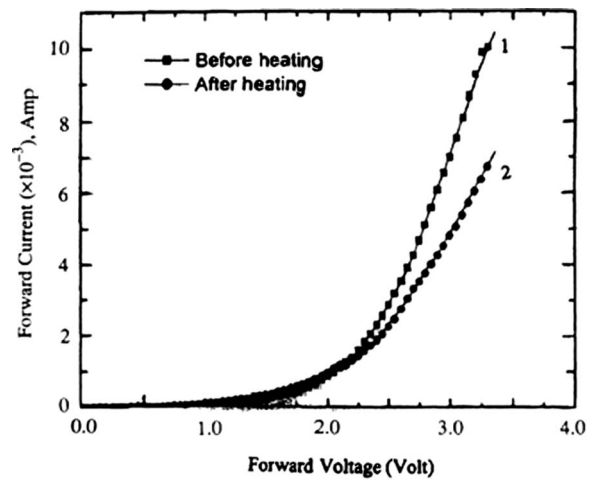


FIG. 4. Forward current-voltage characteristics of  $\text{Al}_x\text{Ga}_{1-x}\text{N}/\text{GaN}$  Schottky diodes before and after heating; curve 1 was obtained for the diodes before heating, and curve 2 was obtained for the diodes after heating, both at room temperature.

Ni/Au partial oxidation, and/or metal interdiffusion, which did not allow  $I_F$ ,  $n_{\text{idl}}$ , and  $\phi_B$  to revert back to the original value. The modification of interface states resulted also from the relaxation of strain of the  $\text{Al}_x\text{Ga}_{1-x}\text{N}/\text{GaN}$  heterostructure, formation of alloys, and change in  $\phi_B$  due to annealing. There are ambiguities in x-ray diffraction patterns obtained for Au/Ni/GaN contacts alloyed at various temperatures.<sup>9</sup> Nevertheless, subject to further investigation, the primary products might have been  $\text{Ni}_3\text{N}$  and  $\text{Ni}_4\text{N}$  for an alloying temperature of  $0^\circ\text{C} < T_{\text{RTA}} < 200^\circ\text{C}$ . The primary products might have been  $\text{Ga}_4\text{Ni}_3$ ,  $\text{Ga}_3\text{Ni}_2$ ,  $\text{Ni}_3\text{N}$ ,  $\text{GaAu}$ , and  $\text{GaAu}_2$  for the alloying temperature of  $500^\circ\text{C} < T_{\text{RTA}} < 600^\circ\text{C}$ .

In conclusion, investigations have been made to highlight the Schottky characteristics of various diodes. While the highest ideality factor for the S2 diodes at  $300^\circ\text{C}$  is about 2.7, the highest ideality factor for the S3 diodes at  $300\text{ K}$  is about 2.1. This indicates that, at various  $T$ , the carrier transport in both the diodes is dominated by thermionic emission. Any deviation from thermionic characteristics is due to recombination and leakage. The most striking feature of our measurements is that they appear to successfully establish the validity of the Schottky-Mott rule for the S1 and S2 diodes and the invalidity of this rule for the S3 diodes.

<sup>1</sup>D. Qiao, L. S. Yu, S. S. Lau, J. M. Redwing, J. Y. Lin, and X. H. Jiang, Appl. Phys. Lett. **87**, 801 (2000).

<sup>2</sup>A. Motayed and S. N. Mohammad, J. Chem. Phys. **123**, 194703 (2005).

<sup>3</sup>Walter Schottky, Naturwiss. **26**, 843 (1938); N. F. Mott, Proc. Cambridge Philos. Soc. **34**, 568 (1938).

<sup>4</sup>C. Lu, H. Chen, X. Lv, X. Xie, and S. N. Mohammad, J. Appl. Phys. **91**, 9218 (2002); A. Motayed, A. K. Sharma, K. A. Jones, M. A. Derenge, A. A. Iliadis, and S. N. Mohammad, *ibid.* **96**, 3286 (2004).

<sup>5</sup>Uwe Karrer, Ph.D. thesis, Walter Schottky Institute Technische Universität München, 2003.

<sup>6</sup>S.-Y. Chen and J.-T. Lue, New J. Phys. **4**, 79.1 (2002).

<sup>7</sup>H. Tiesseyre, P. Perlin, T. Suski, A. Pietraszko, and T. D. Moustakas, J. Appl. Phys. **76**, 2429 (1994); Q. Guo and A. Yoshida, Jpn. J. Appl. Phys., Part 1 **33**, 2453 (1994).

<sup>8</sup>Y. Koide, H. Itoh, M. R. H. Khan, K. Hiramatsu, N. Sawaki, and I. Akasaki, J. Appl. Phys. **61**, 4540 (1987).

<sup>9</sup>J. D. Guo, F. M. Pan, M. S. Feng, R. J. Guo, P. F. Chou, and C. Y. Chang, J. Appl. Phys. **80**, 1623 (1996); J. K. Sheu, Y. K. Su, G. C. Chi, W. C. Chen, C. Y. Chen, C. N. Huang, J. M. Hong, Y. C. Yu, C. W. Wang, and E. K. Lin, *ibid.* **83**, 3172 (1998).